



miR-132 downregulation alleviates behavioral impairment of rats exposed to single prolonged stress, reduces the level of apoptosis in PFC, and upregulates the expression of MeCP2 and BDNF

Lei Tong^a, Ming-Da Li^b, Peng-Yin Nie^a, Yao Chen^a, Yu-Lu Chen^a, Li-Li Ji^{a,*}

^a Department of Anatomy, College of Basic Medical Sciences, China Medical University, Shenyang, China

^b Department of 1st Clinical Medicine, China Medical University, Shenyang, China

ARTICLE INFO

Keywords:

Post-traumatic stress disorder
miR-132
MeCP2
BDNF
Anxiety-like behavior

ABSTRACT

Post-traumatic stress disorder (PTSD) is usually accompanied by anxiety symptoms and decreased expression of brain-derived neurotrophic factor (BDNF), which played an important role in promoting neuronal proliferation and survival. Methyl CpG-binding protein 2 (MeCP2) is a positive mediator of BDNF and is regulated by miR-132-3p. In the present study, we explored the possible molecular mechanism of miR-132, focusing on the involvement of MeCP2 and BDNF in the formation of anxiety-like symptoms of PTSD. Single prolonged stress (SPS) was used to establish a model of PTSD in adult rats and the anxiety-like behavior was tested by the elevated plus-maze (EPM). The level of miR-132 in the prefrontal cortex (PFC) was increased and intraventricular injection of anti-miR-132 could significantly improve the anxiety-like behavior of rats exposed to SPS through MeCP2 and the subsequent upregulation of BDNF levels. Then tropomyosin-related kinase B (TrkB) and downstream signals, including MAP kinase ERK1/2 and phosphoinositol 3-kinase (PI3K)/Akt pathways, were activated by BDNF upregulation, and might participate in regulating dendritic complexity and the expression of postsynaptic density-95 (PSD95) and synapsin I in the PFC of SPS rats. Furthermore, we found that the apoptosis of cells in PFC induced by SPS procedure could be alleviated by miR-132 inhibition. Our results suggest that miR-132 might be involved in the formation of anxiety-like symptoms of adult rat PTSD models by targeting MeCP2, and this effect is related to BDNF/TrkB and its downstream ERK and Akt signaling pathways.

1. Introduction

Post-traumatic stress disorder (PTSD) is a psychiatric disorder characterized by symptoms of persistent anxiety after experiencing traumatic events, such as sexual assault, life-threatening injury, emotional trauma, severe accidents or brutal physical assaults (Cosen-tino et al., 2019; Kessler et al., 1995). The disorder may manifest itself through a variety of symptoms, including mood (e.g., depression, anxiety), cognition (e.g., flashbacks, nightmares) and emotion (e.g., mental instability, impulsivity, and hyperarousal), and impaired social skills (Bitencourt and Takahashi, 2018; Jurkus et al., 2016). Several symptoms, such as anxiety arousal, nightmares, flashbacks, emotional/physiologic reactivity, are related to the tendency to treat neutral stimuli as threats, increased generalization of fear, deficits in fear extinction, and changes in the processing of threatening environments. These abnormalities are caused by neuropathies that impair the functional

connectivity of the brain, such as the anterior cingulate cortex (ACC), prefrontal cortex (PFC), hippocampus and amygdala (Armour et al., 2016; Briscione et al., 2014; Bromis et al., 2018; Dossi et al., 2020; Krystal et al., 2017). Increased anxiety-like behavior is one of the important hallmark symptoms of PTSD. However, the molecular mechanism of the pathogenesis of PTSD has not been clearly studied, and the treatment of PTSD is also extremely challenging, which may include years of individual and group research and drug treatment. The study of the molecular mechanism of PTSD may be one of the methods to find a suitable therapeutic target for PTSD.

MicroRNAs (miRNAs), the translation regulators that act by initiating the degradation of messenger RNA and translational repression, are frequently dysregulated in many diseases, including several neuropsychiatric and neurodegenerative disorders, such as major depressive disorder (MDD), Alzheimer's disease (AD) and Parkinson's disease (PD) (Doxakis, 2010; Eacker et al., 2013; Femminella et al., 2015; Shukla

* Corresponding author.

E-mail address: ljji@cmu.edu.cn (L.-L. Ji).

<https://doi.org/10.1016/j.ynstr.2021.100311>

Received 17 December 2020; Received in revised form 1 February 2021; Accepted 19 February 2021

Available online 25 February 2021

2352-2895/© 2021 Published by Elsevier Inc. This is an open access article under the CC BY-NC-ND license (<http://creativecommons.org/licenses/by-nc-nd/4.0/>).

et al., 2011; Smalheiser et al., 2012). It also has been reported that miRNAs are related to the pathophysiology of PTSD and can be used as potential biomarkers (Snijders et al., 2018). MiRNAs are widely expressed in the central nervous system (CNS) and play a key role in dendritic development, axon outgrowth and branching, and synaptic plasticity (Dajas-Bailador et al., 2012; Hu and Li, 2017; Magill et al., 2010). MiR-132 is one of the miRNAs widely present in the CNS, and regulates dendrite morphology and synapse function through its target genes, methyl CpG-binding protein 2 (MeCP2) and Rho GTPase activator p250GAP (Klein et al., 2007; Siegel et al., 2011; Wanet et al., 2012; Wayman et al., 2008). Our previous studies have shown that the level of miR-132 in the hippocampus of rats is significantly increased following single prolonged stress (SPS), and the downregulation of miR-132 may increase the expression of synapse-related proteins through its target gene Fragile X-related protein 1 (FXR1), including postsynaptic density-95 (PSD95) and synapsin I in hippocampal neurons (Nie et al., 2020). However, it is not clear whether miR-132 is involved in the pathogenesis of PTSD by regulating other target genes (such as MeCP2).

Brain-derived neurotrophic factor (BDNF) has emerged as an important downstream mediator of MeCP2 and an indirect target of miR-132 (Chen et al., 2003; Martinowich et al., 2003). BDNF mainly binds to the high-affinity receptor tyrosine kinase tropomyosin-related kinase B (TrkB), and recruits transcriptional and translational mechanisms via initiating an intracellular downstream signaling, including MAP kinase ERK1/2 and phosphoinositol 3-kinase (PI3K)/Akt pathways (Huang and Reichardt, 2003). The BDNF-TrkB signaling cascade and its downstream transcriptional effectors, ERK or Akt, are highly correlated with synaptic plasticity (Roskoski, 2012; Silva-Pena et al., 2019). Stress, such as chronic stress and PTSD, may impair the integrity of signaling through glutamate synapses in a variety of ways, including reducing signaling through BDNF and weakening its downstream intracellular signaling, thus resulting in decreased dendritic complexity (Krystal et al., 2017). These deficits in structural connectivity are associated with cognitive impairments, which are symptoms of PTSD (Nicholson et al., 2016). We propose that miR-132 has a necessary and sufficient effect on stimulating dendritic spines activity and neuronal complexity in PTSD rats by targeting MeCP2. MeCP2 may further regulate BDNF and its downstream signaling pathways, thereby participates in the pathophysiological process of anxiety-like symptoms of PTSD.

In the present study, we investigated the aberrant expression of miR-132 and its downstream target MeCP2 in rat PFC, as this region has been shown to play a major role in increased vulnerability to stress when exposed to SPS paradigm. We also explored whether miR-132 downregulation was involved in alleviating anxiety-like behaviors in rats exposed to SPS by the injection of a lentivirus-delivered miR-132 inhibitor. Furthermore, we examined the levels of BDNF, TrkB, p-ERK, p-Akt, PSD95, synapsin I proteins and apoptotic level of cells in PFC to explore the possible mechanism of miR-132 in regulating anxiety-like behavior in rats exposed to SPS.

2. Materials and methods

2.1. Animals, single-prolonged stress (SPS) paradigm and experimental groups

Sixty Sprague-Dawley (SD) rats (male, 3–4 months old, weighing 200–250g) were purchased from the Experimental Animal Center of China Medical University and fed under standard laboratory conditions with an air humidity range of 40%–60%, constant temperature range of 22 °C–26 °C, and water and food freely available under a 12-h light/dark cycle for a week. The experiments were in accordance with the guidelines for the Care and Use of Laboratory Animals from the National Institutes of Health, and were approved by the animal welfare committee of China Medical University.

The rats were divided into SPS group (n = 54), in which the rats received the SPS procedure and Control group (n = 18), in which the rats

were fed normally. The SPS paradigm was as we described previously. Briefly, the rats were confined in the plastic containers (58 mm in diameter, 150 mm in length), and then forced to swim for 20 min respectively. After resting for 15 min, the rats were exposed to diethyl ether until they were unconscious. Then the rats in the SPS group were further divided into 4 groups according to the different substances injected into the lateral ventricle: SPS group, Sh-miR-NC group, Sh-miR group and miR group. The latter three groups were treated with the scramble control lentivirus (LV-NC), lentivirus-encoding reverse complementary sequence of miR-132 and lentivirus-encoding miR-132, respectively.

2.2. Injection of the lentiviral-mediated miR-132-3p inhibitor

The rats were anesthetized by intraperitoneal injection of sodium pentobarbital and then the lentiviral-encoding miR-132-3p (Lv-miR-132, Wanlei Biotech Co., Ltd.; Shenyang, China) or lentiviral-encoding reverse complementary sequence of miR-132-3p (LV-anti-miR-132, Wanlei Biotech) or the scramble control (Lv-NC, Wanlei Biotech) was injected into the right lateral ventricle of rats via stereotaxic device according to the following coordinates: A/P (bregma): −1.2 mm; M/L (laterality): +2.0 mm; D/V (depth): −4.0 mm. The final titer of the vector was 1×10^8 TU/mL and it was injected at a dose of 10 μ L per rat 7 days after the SPS procedure.

2.3. Elevated plus-maze

Anxiety-like behavior of animals was evaluated using the elevated plus-maze (EPM) test. The EPM was made of black fiberboard with a four-arm platform, including a pair of open arms and a pair of close arms (length 50 cm and width 10 cm respectively), and was raised about 50 cm from the ground. The test was carried out as follows: each rat was placed in the central area (10 × 10 cm) with its head positioned toward the open arm and its behavior within 5 min was recorded with a camera. 75% alcohol was sprayed on the EPM platform between two sessions to avoid odor effects. The retention time in open or close arms and the number of times the animal entered the two arms were recorded separately within 5 min by an automatic image analysis system (Xinruan Information Technology Co. Ltd, Shanghai, China).

2.4. Immunofluorescence staining

The rats in each group were anesthetized by intraperitoneal injection of sodium pentobarbital and the brains were removed and incubated in 4 °C paraformaldehyde overnight. After precipitation in 15%, 25%, and 30% sucrose solution for 24 h respectively, the brain tissue was sliced with a cryostat with a thickness of 7 μ m. The sections were stored at −20 °C and taken out 2 h before immunofluorescence staining. The immunofluorescence staining was carried out as follows: The sections were washed three times by 0.1M phosphate buffer saline (PBS), permeabilized in 0.2% Triton X-100 for 30 min, and blocked with 5% fetal bovine serum (FBS) for 2 h at room temperature. The tissues were then incubated with chicken MAP-2 (1:500, Abcam, Cambridge, MA, USA), rabbit PSD95 (1:200, Abcam) primary antibodies at 4 °C overnight. After washing three times by PBS, the tissues were incubated with donkey anti-chicken 488-conjugated secondary antibody (1:600; Abcam) and donkey anti-rabbit 594-conjugated secondary antibody (1:600; Abcam) for an hour at 37 °C. 4', 6-diamidino-2-phenylindole (DAPI) was used to stain the nuclei. Omission of the primary antibody in parallel staining was used as a control to ensure no non-specific staining. Images were taken with an Olympus BX51 microscope.

2.5. Neuron-like cell culture and transfection

Neuron-like cells were induced from PC12 cells treated with DMEM/F12 (Gibco, Thermo Fisher Scientific Inc., USA) containing 100 ng/mL

nerve growth factor (NGF, R&D Systems Inc., USA) for 24 h. Five microliters lentivirus-encoding reverse complementary sequence of miR-132-3p (LV-miR-132), with a titer of 1×10^8 TU/ml, was added to 200 μ L of neuron-like cell culture medium, and the transfection efficiency was observed with a fluorescence microscope 3 days after transfection. The total protein and mRNA of cells were extracted, and the levels of MeCP2 or BDNF protein and mRNA were tested by western blotting and RT-qPCR, respectively.

2.6. Western blotting

The PFCs of rats in each group were separated and weighed with an electronic balance. The tissue was cut into pieces with scissors, washed 3 times with saline, and dissolved in a mixture of RIPA buffer and 2 mM PMSF (Beyotime Biotech, Shanghai, China). The protein concentration was determined using the BCA protein assay kit (Beyotime). Then the protein was diluted with PBS and loading buffer and boiled for 5 min. 30 μ g total protein in each group was electrophoretically separated by 8% or 10% sodium dodecyl sulfate-polyacrylamide (SDS-PAGE) gels, and incubated at 4 °C overnight with primary antibodies as follows: rabbit MeCP2 (1:5000, Abcam), rabbit BDNF (1:1000, Abcam), rabbit TrkB (1:1000, Abcam), rabbit PSD95 (1:1000, Abcam), rabbit ERK (1:2000, Abcam), rabbit p-ERK (1:1000, Abcam), rabbit Akt (1:2000, Abcam), rabbit p-Akt (1:1000, Abcam) and rabbit GAPDH (1:8000; Proteintech). The membrane was washed three times in TBST, and then incubated with HRP- conjugated goat anti-rabbit IgG (1:10000; Proteintech) at 37 °C for another 1 h, followed by ECL detection and imaging using a Bio-Rad ChemiDoc imaging system (Bio-Rad).

2.7. Reverse transcription quantitative Real-time PCR (RT-qPCR)

Total RNA was isolated from PFC of rats in each group using Total RNA Isolation Kit (Vazyme Biotech, Nanjing, China) according to manufacturer's protocol. A total of 1 μ g RNA was used for reverse transcription (RT) using miRNA 1st strand cDNA synthesis kit (Vazyme Biotech), followed by an amplification reaction using the StepOnePlus system (Applied Biosystems, USA) with corresponding primers obtained from Sangon Biotech (Shanghai, China). MiR-132 level was normalized to U6, and MeCP2 and BDNF mRNA levels were normalized to GAPDH. The fold change was based on the $2^{-\Delta\Delta Ct}$ method with 3 sample repetitions for each group. The primer sequences were as shown in Table 1.

2.8. Dual luciferase reporter assay

Dual luciferase reporter assay was used to further confirm the binding of miR-132-3p to MeCP2 mRNA. HEK 293 T cells were cultured in 24-well plates and co-transfected with miR-132 mimic, and wild-type MeCP2 3'UTR reporter plasmid (pmiR- MeCP2-wt) or mutant MeCP2 3'UTR reporter plasmid (pmiR-MeCP2-mut), synthesized by GenPharma (Shanghai, China). The medium was refreshed with fresh

Table 1
Oligonucleotide sequences of primers.

Gene	Upstream	Downstream
miR-132	5'- GGGCGTAACAGTCTACAGCCA-3'	5'- AGTGCAGGGTCCGAGGTATT-3'
U6	5'-CTCGCTTCGGCAGCACATA-3'	5'- AACGATTACACGAATTTGCGT-3'
BDNF	5'-CCTGGTGAACITCTTTGGGG-3'	5'- GAAAGCGAGCCCGATTGG-3'
PSD95	5'-TACCAAAGACCGTGCCAACG-3'	5'-CGGCATTGGCTGAGACATCA-3'
Synapsin I	5'- GTGTCAGGGAACCTGGAAGACC-3'	5'-AGGAGCCACCACTCAATA-3'
GAPDH	5'-ACGCCAGTAGACTCCACGAC-3'	5'-ATGACTTACCCACGGCAAG-3'

medium supplemented with 10% FBS after incubation with the transfection reagent/DNA complex for 3 h. 48 h after transfection, the Dual Luciferase Reporter Gene Assay kit (Promega, USA) was used to determine the luciferase activities of each group.

2.9. Golgi staining

The brain of rats was removed and fixed in 2% PFA/2.5% glutaraldehyde for more than 24 h and then was sectioned (100 μ m) using a vibratome. Then the slices were stained with the Rapid Golgi protocol as previously described (Lee et al., 2004). Basal dendrites were randomly selected for imaging and the dendritic spine density was calculated as spines number per 10 mm dendritic length from the soma.

2.10. Flow cytometry

The levels of apoptosis in neurons of PFC were evaluated by PE Annexin V Apoptosis Detection Kit (BD Biosciences, Burlington, MA, USA) according to manufacturer's instruction. Briefly, the PFC of rats in the Control, SPS and Sh-miR groups were dissected into single-cell suspension. Cells were resuspended by binding buffer at a concentration of 1×10^6 cells/ml after being washed twice with cold PBS. The mixture of 5 μ l phycoerythrin (PE)-labeled Annexin V and 5 μ l 7-aminocincomycin D (7-AAD) was added into the culture tube and the cells were gently vortexed. Then the cells were incubated for 15 min at room temperature under dark condition. The apoptotic cells were analyzed with a FACSCalibur flow cytometer after adding 400 μ l binding buffer. The PE-labeled Annexin V positive cells were considered to be apoptotic cells.

2.11. Statistical analysis

The data are expressed as the mean \pm SEM, and analyzed by SPSS19.0 statistical software. Independent samples *t*-test was used to compare data between two groups. One-way analysis of variance (ANOVA) with post hoc S-N-K test analysis was used to compare more than three groups of data. *P* value < 0.05 is considered a significant difference, and is indicated by the symbol * in the figures.

3. Results

3.1. The levels of MeCP2 and BDNF in the rat PFC following SPS procedure

Antisense miR-132 delivered by LV-anti-miR-132 was injected into the right lateral ventricle of rats 7 days after SPS procedure, and EPM test was performed 7 days after injection. The rats were sacrificed at different time points in each experimental procedure, as shown in Fig. 1A. One day after EPM test, the level of miR-132 in rat PFC of the Control and SPS groups was measured by RT-qPCR analysis (Fig. 1B, $t = 4.803$, $P = 0.0049$). Our previous study showed that the level of miR-132 in the hippocampus of SPS rats was significantly increased, and miR-132 downregulation could significantly alleviate PTSD-like symptoms in rats, but the mechanism has not been clearly studied (Nie et al., 2020). MeCP2 was found to be a target gene of miR-132 through bioinformatics analysis (www.targetscan.org), and was involved in dendritic growth, spine maturation and BDNF gene expression (Zhou et al., 2006). In this study, we detected the levels of MeCP2 and BDNF by western blot and found that their levels were significantly decreased in the PFC of SPS rats (MeCP2: Fig. 1C and D, $t = 1.013$; BDNF: Fig. 1C and E, $t = 3.358$). These results indicated that miR-132 might participate in the pathogenesis of PTSD rats through MeCP2 and BDNF.

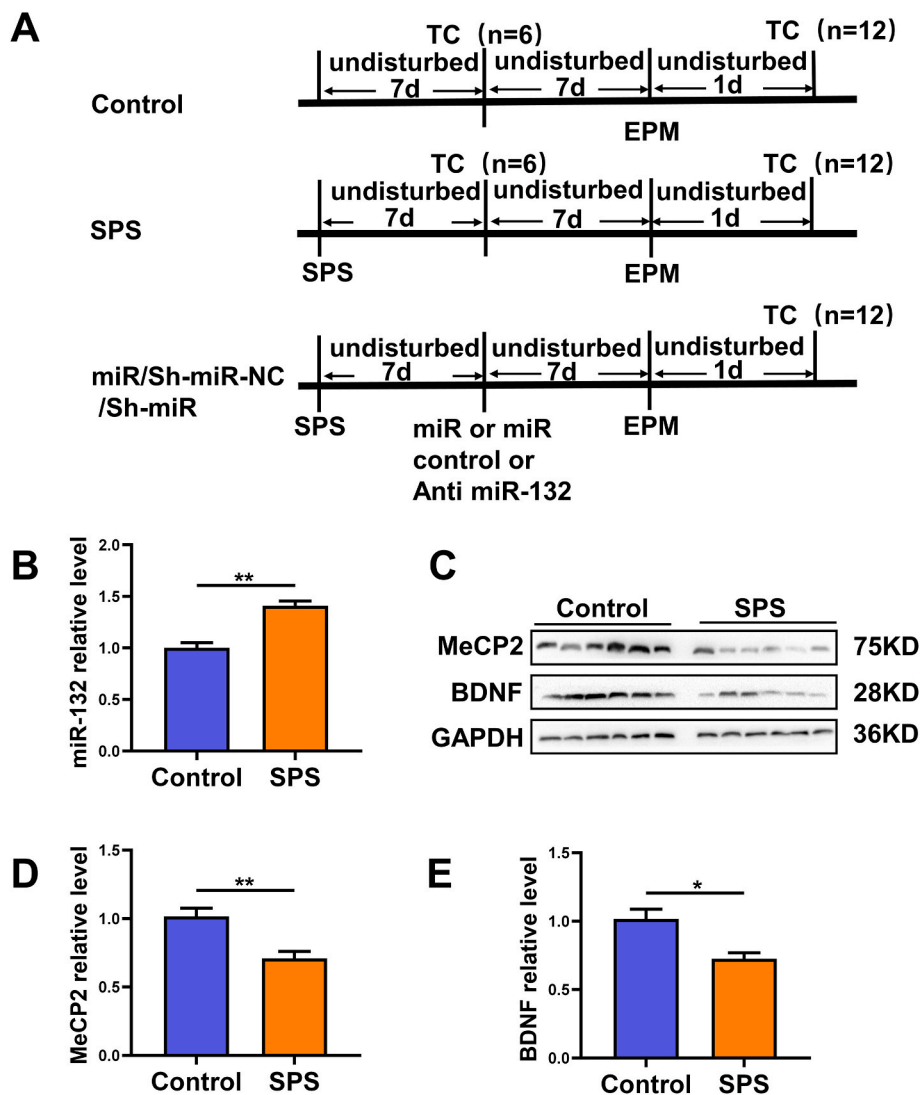


Fig. 1. The levels of MeCP2 and BDNF in the PFC of rats exposed to SPS. (A) The experimental procedure in this study. (B) The relative level of miR-132 in the prefrontal cortex (PFC) of rats exposed to SPS. (C) Representative western blot images. The relative levels of (D) MeCP2 and (E) BDNF in the Control group and SPS group. The data represent the means \pm standard errors of the mean (SEM) with 6 rats per group. Glyceraldehyde 3-phosphate dehydrogenase (GAPDH) was used as a loading control. * $P < 0.05$, ** $P < 0.01$.

3.2. Downregulation of miR-132 target genes expression in the neuron-like cells

As mentioned above, MeCP2 was a target of miR-132 predicted by bioinformatics analysis, which could directly regulate the level of BDNF. Therefore, we explored whether miR-132 overexpression could regulate the levels of MeCP2 or BDNF. LV-anti-miR-132-3p labeled with green fluorescent protein (Lv-GFP-miR) was transfected into the neuron-like cells and induced by PC-12 cells treated with 100 ng/mL NGF for 24 h. The levels of MeCP2 or BDNF were detected by western blot. Both MeCP2 and BDNF protein expression was decreased significantly by the overexpression of miR-132 (MeCP2: Fig. 2B and C, $t = 5.282$; $P = 0.0340$; BDNF: Fig. 2B and D, $t = 4.900$; $P = 0.0392$). We further detected the BDNF mRNA level through RT-qPCR and found that the overexpression of miR-132 significantly decreased the level of BDNF mRNA (Fig. 2E, $t = 3.199$; $P = 0.0240$). These results showed that miR-132 overexpression could downregulate the MeCP2 and BDNF protein expression and the level of BDNF mRNA.

This result suggested that miR-132 might inhibit the expression of MeCP2, which was one of target genes of miR-132 predicted by bioinformatics analysis. The 3'-UTR region of MeCP2 has a binding site to miR-132-3p, which contained conservative seed sequence at position 6705–6712 (Fig. 2F). In order to confirm whether miR-132-3p binds to MeCP2 mRNA, we further carried out a dual-luciferase reporter assay.

We constructed the 3'-UTR of MeCP2 encompassing miR binding sites downstream of the firefly luciferase gene. The result showed that the relative luciferase activity was significantly decreased in HEK 293 T cells co-transfected with the wild-type vector and enhanced miR-132 expression (Fig. 2G; $p < 0.001$), and there was no reduction when the miR-132 seed sequence was mutated.

In order to study whether the level of BDNF was regulated by MeCP2, we evaluated the expression level of BDNF in the neuron-like cells transfected by MeCP2 or sh-MeCP2. Compared to the cells in the Control group, the expression level of BDNF in the MeCP2 group was significantly increased, while the level was decreased significantly in the sh-MeCP2 group (Fig. 2H and I, $F(2, 6) = 32.44$, $P = 0.0006$).

These results suggested that MeCP2 was a direct target of miR-132, and miR-132 could inhibit the expression of MeCP2 through binding to the 3'-UTR site of it. In addition, miR-132 might regulate the expression of BDNF by binding to MeCP2 mRNA.

3.3. The effects of miR-132 downregulation on the anxiety-like behavior

In order to explore whether miR-132 was involved in regulating the anxiety-like behavior of rats exposed to SPS procedure, we examined the behavior of rats through EPM test after the injection miR-132 or anti-miR-132. The results showed that, compared with the Control group, the rats in the SPS group spent less time in the open arms and entered the

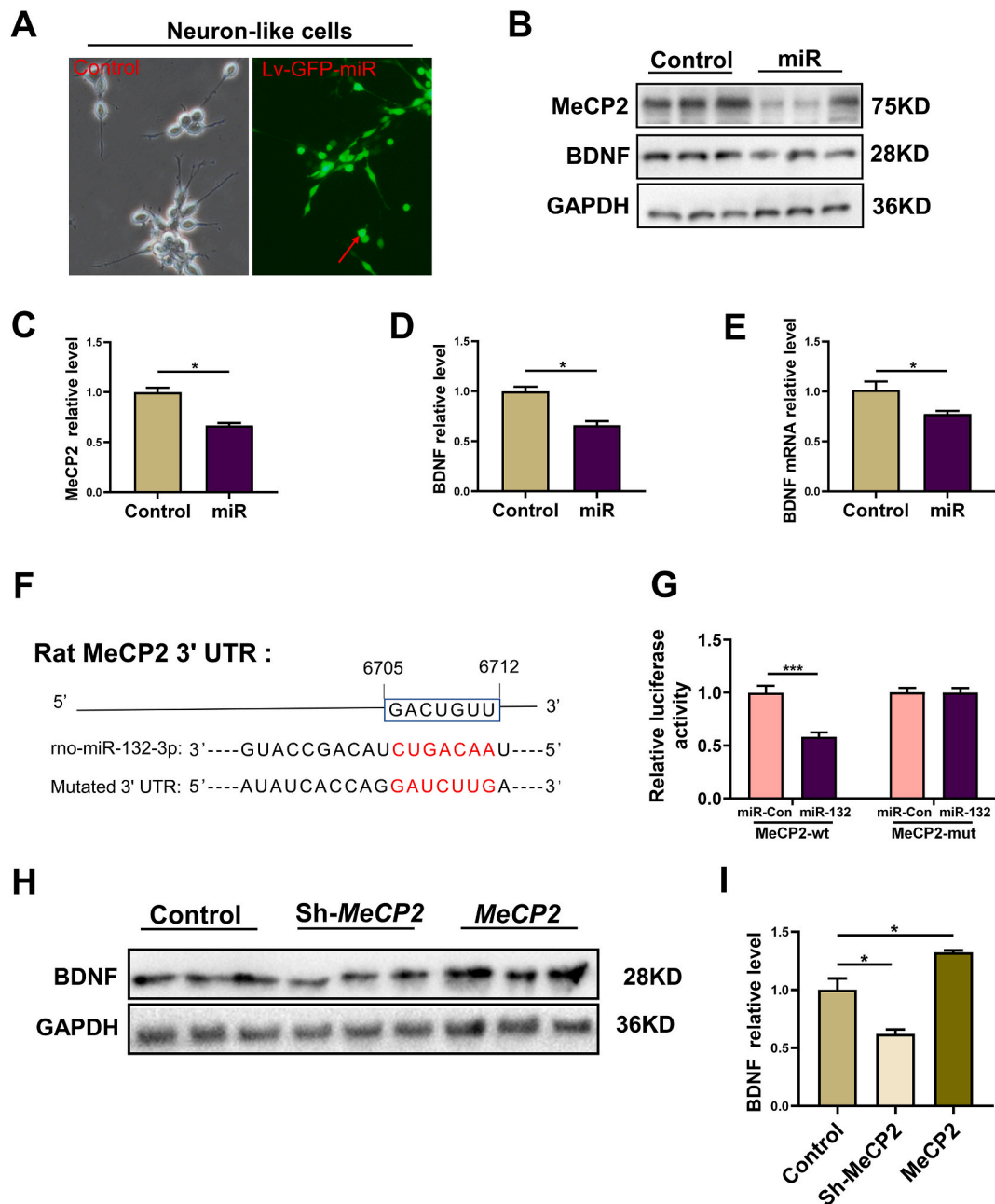


Fig. 2. The effect of miR-132 overexpression on MeCP2 and BDNF levels in the neuron-like cells. (A) Representative images of cultured and miR-132 transfected PC-12 cells treated with NGF. (B) Representative Western blot bands of MeCP2 and BDNF protein in cultured and miR-132 transfected PC-12 cells treated with NGF. GAPDH was used as a loading control. The relative level of (C) MeCP2 and (D) BDNF in each group. (E) The mRNA level of BDNF tested via RT-qPCR. (F) Schematic illustration indicating the conserved seed match of MeCP2 3'UTR of miR-132-3p. (G) Relative luciferase activity as expressed with firefly/Renilla luciferase activity. Luciferase was fused to the 3'UTR of MeCP2 containing a wild type or a mutated seed site in the presence of miR-control or miR-132-3p. (H) Representative BDNF protein bands in cultured PC-12 cells treated with NGF which transfected with Sh-MeCP2 or MeCP2 tested by Western blot. (I) The relative level of BDNF in each group. The data represent the means \pm standard errors of the mean (SEM). * $P < 0.05$, *** $P < 0.001$.

open arms less frequently. However, this trend could be reversed by anti-miR-132 injection (Open arm time: Fig. 3B, $F(3, 25) = 7.807$, $P = 0.0003$; Open arm entries: Fig. 3C, $F(3, 25) = 8.437$, $P = 0.0002$). Interestingly, intracerebroventricular injection of miR-132 did not affect the anxiety-like behavior of rats. These results indicated that rats exposed to SPS procedure significantly increased anxiety-like behavior, which could be alleviated by anti-miR-132 injection through the lateral ventricle.

3.4. The effects of anti-miR-132 on the expression of MeCP2 and BDNF

To investigate the possible mechanism of intracerebroventricular injection of anti-miR-132 on alleviating anxiety-like behavior in rats exposed to SPS procedure, we tested the expression level of MeCP2, whose mRNA was predicted as a target gene of miR-132-3p. LV-anti-miR-132 was injected into the right lateral ventricle of rats and the transfection efficiency was tested by RT-qPCR (Fig. 4A, $t = 4.500$, $P = 0.046$). We found that the level of MeCP2 protein was significantly decreased in the PFC of SPS rats, while this trend was reversed by anti-miR-132 (Fig. 4B, $F(3, 25) = 15.62$, $P < 0.0001$), consistent with the

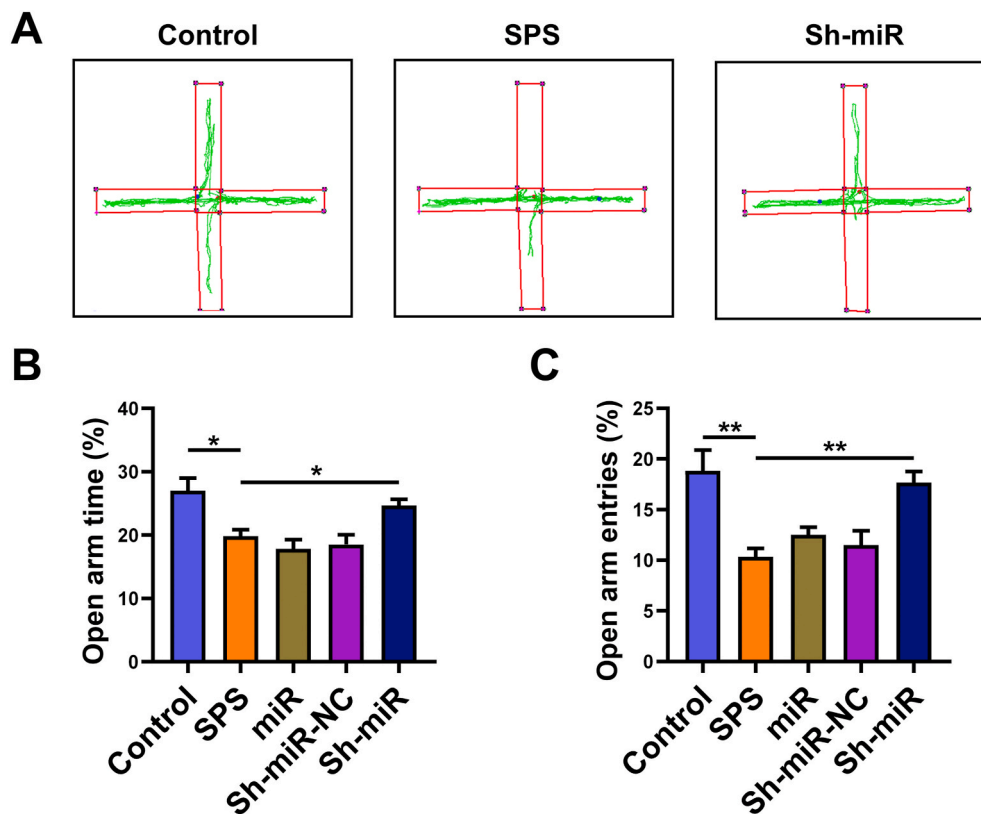


Fig. 3. The effect of anti-miR-132 injection on the anxiety-like behavior of rats exposed to the SPS procedure. (A) Representative walking track of rat in the Control, SPS and Sh-miR groups by the EPM test. (B) Open arm time and (C) open arm entries of rats in the EPM test. The data represent the means \pm standard errors of the mean (SEM) with 6 rats per group. * $P < 0.05$, ** $P < 0.01$.

results we got above that miR-132 downregulation could increase the MeCP2 level in cultured neuron-like cells.

We further tested the level of BDNF protein in the PFC of rats in each group through western blot to investigate whether miR-132 regulated the expression of BDNF. We found that the level of BDNF in the SPS group was significantly decreased and this trend could be reversed by anti-miR-132 injection (Fig. 4C, $F(3, 25) = 6.916$, $P = 0.0007$). The expression of BDNF was then evaluated by duo-immunofluorescence with the neuron-specific marker MAP2. The rats exposed to SPS exhibited reduced BDNF expression in the PFC compared with the Control group and anti-miR-132 could reverse this trend (Fig. 4E).

These results were consistent with the point that BDNF was regulated by MeCP2 directly and positively and might be considered as an indirect target of miR-132. However, unlike the effect on cells, the injection of miR-132 did not further affect the expression of BDNF in the PFC of rats exposed to SPS.

3.5. The effects of anti-miR-132 on the TrkB, ERK and Akt expression in PFC

We also examined the effect of anti-miR-132 on TrkB, a receptor of BDNF, and its signaling molecule ERK and Akt in the PFC of rats in the Control, SPS and Sh-miR group. As shown in Fig. 5A and B, the expression of TrkB in the PFC of rats was significantly downregulated by the SPS procedure, while it was reversed by anti-miR-132 ($F(2, 15) = 7.267$, $P = 0.0062$). The interaction of TrkB and BDNF could promote neuronal differentiation, growth and survival through activation of ERK and Akt (Minichiello, 2009). We next examined the activation of ERK and Akt, and the results showed that the levels of both p-ERK (phosphorylated ERK) and p-Akt (phosphorylated Akt) were significantly decreased in the PFC of SPS rats, compared to that in the Control group. However, these trends were rescued by anti-sh-miR-132 injection

(p-ERK: Fig. 5D, $F(2, 15) = 8.263$, $P = 0.0038$; p-Akt: Fig. 5F, $F(2, 15) = 10.67$, $P = 0.0013$). These results indicated that anti-miR-132 might rescue the downregulation of BDNF and TrkB levels in the PFC induced by the SPS procedure and activate the ERK and Akt pathway, thereby alleviate the anxiety-like behavior of rats exposed to SPS.

3.6. The effects of anti-miR-132 on PSD95 expression in the PFC of SPS rats

Next, we examined the level of PSD95 to explore the effect of anti-miR-132 on neurons in the PFC, for PSD95 and synapsin I were crucial for morphological maturation and synaptic development of neurons. The results showed that the levels of PSD95 and synapsin I in the PFC was significantly decreased by the SPS procedure in the SPS group, compared to the Control group, but this trend was also reversed by anti-miR-132 (PSD95: Fig. 6B and C, $F(2, 15) = 5.824$, $P = 0.0134$; synapsin I: Fig. 6B and D, $F(2, 15) = 11.4$, $P = 0.0010$). Then we further tested the mRNA levels of PSD95 and synapsin I, and the results were consistent with that in Western blot (PSD95: Fig. 6E and F, $F(2, 15) = 9.429$, $P = 0.0022$; synapsin I: Fig. 6F, $F(2, 15) = 11.16$, $P = 0.0011$).

Dendritic spines are small membrane protrusions on dendrites and play critical roles in the synaptic formation and neural circuits. We further detected the effect of miR-132 inhibition on dendritic spines through Golgi staining, and the morphology of neurons in the PFC was shown in Fig. 7A. The density of dendritic spines was decreased in the PFC neurons of rats exposed to SPS, and anti-miR-132 could significantly reverse this trend. The spine number in the dendrites of PFC neurons in the rats exposed to SPS was significantly decreased and this trend could be reversed by the miR-132 inhibitor injection (Fig. 7B, $F(2, 15) = 9.530$, $P = 0.0021$).

These results provided evidence that anti-miR-132 not only regulated the expression of synaptic protein PSD95 and synapsin I, but also

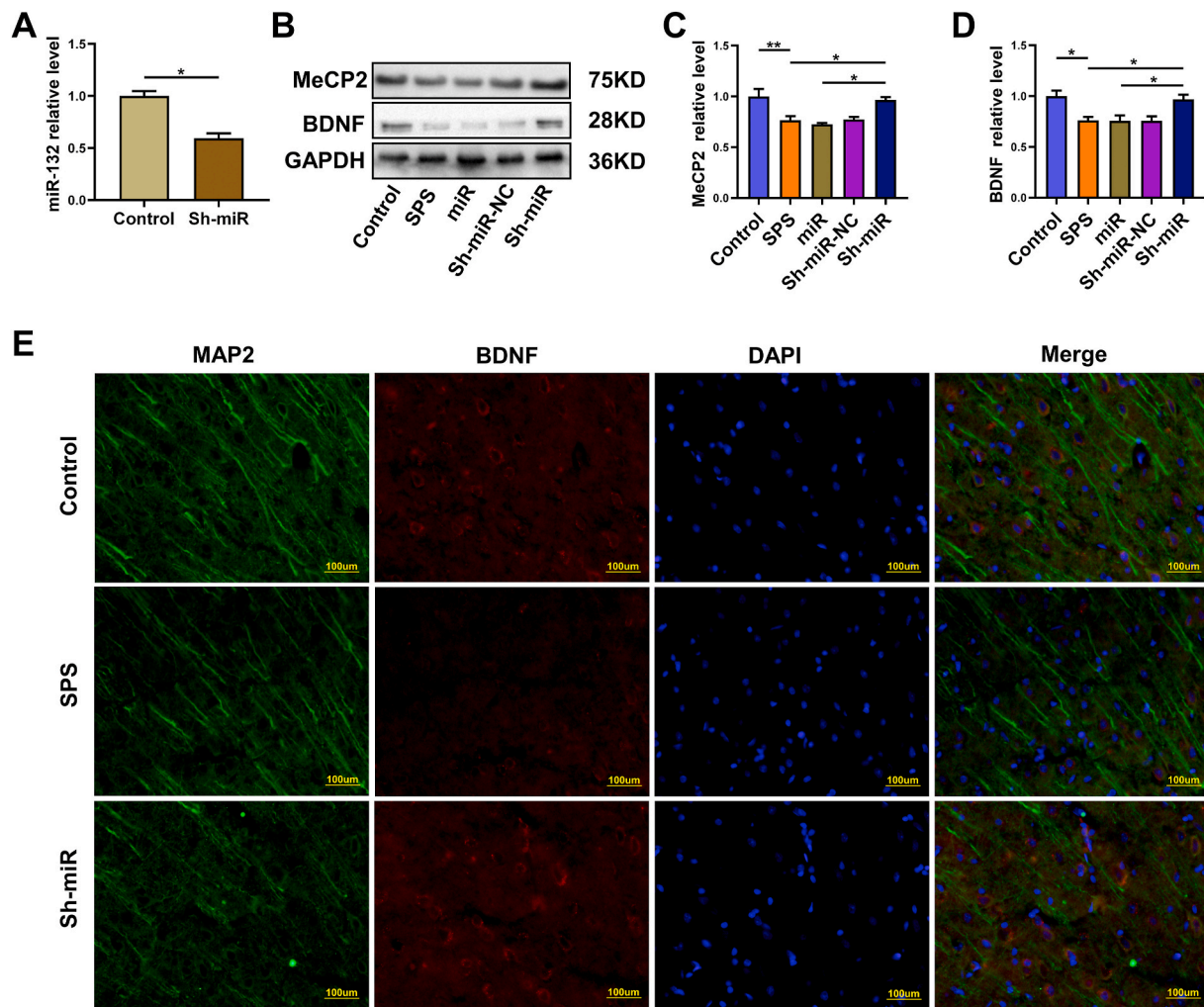


Fig. 4. The effect of anti-miR-132 on the MeCP2 and BDNF expression in PFC of rats in each group. (A) MiR-132 level in PFC of rats in Control and Sh-miR group which were transfected anti-miR-132. The data represent the means \pm standard errors of the mean (SEM) from 3 rats per group. U6 was used as a loading control. (B) Representative images of MeCP2 and BDNF protein in PFC of rats in each group. The relative level of (C) MeCP2 and (D) BDNF in each group. The data represent the means \pm standard errors of the mean (SEM) from 6 rats per group. GAPDH was used as a loading control. * $P < 0.05$, ** $P < 0.01$.

regulated the formation of dendritic spines.

3.7. The effects of miR-132 inhibition on apoptosis of cells in the PFC of rats exposed to SPS

Furthermore, we examined the apoptotic level of neurons in the PFC of rats exposed to the SPS procedure, and whether miR-132 inhibition had an anti-apoptosis effect on the PFC neurons. Here, we tested the expression levels of bcl-2 and bax proteins, which were two homologous proteins with opposite effects on cell life and death. Bcl-2 can prolong cell survival while bax was an accelerator of apoptosis (Matsushita et al., 2000; Reed, 1994). The results showed that the Bcl-2 expression was significantly decreased and the level of Bax was increased in the PFC of SPS rats, and miR-132 inhibition could reverse the trend of these two proteins tested by Western blot (Bcl-2: Fig. 8A and B, $F(3, 20) = 7.392$, $P = 0.0016$; Bax: Fig. 8A and C, $F(3, 20) = 9.822$, $P = 0.0003$). Then we further tested the expression of caspase-3, which was also used as a hallmark of apoptosis. The results indicated that the expression of caspase-3 was significantly upregulated in the PFC of SPS rats. However, the downregulation of miR-132 could reverse this trend significantly (Fig. A and D, $F(3, 20) = 3.27$, $P < 0.0001$). Moreover, we performed Annexin V-FITC/PI double-labeled flow cytometry to assess early apoptosis in the PFC neurons by flow cytometry assay. The percentage of

early apoptotic cells was increased in the PFC of SPS rats, while miR-132 inhibition significantly decreased the percentage of apoptotic cells (Fig. 8E and F (2,15) = 12.55, $P = 0.0006$).

The results above indicated that there was an increased level of cell apoptosis in the PFC of rats, while miR-132 inhibition has an anti-apoptosis effect on the cells of PFC.

4. Discussion

PTSD is a disorder associated with functional impairments, physical health concerns, and mental health comorbidities and is also commonly associated with concurrent anxiety and depression symptoms (Hou et al., 2018; Ni et al., 2020). Both our previous and present studies showed that rats stimulated by SPS showed obvious anxiety and depression-like symptoms, consistent with the results obtained by other researchers (Serova et al., 2019; Wei et al., 2019).

Some studies showed that miRNAs significantly influence the essential cellular processes associated with CNS repair in the CNS diseases including neurodegenerative disorders (Roitbak, 2020; Sillivan et al., 2020). In the present study, we found an increased level of miR-132 in the rat PFC 30 min after exposing to SPS procedure compared to the control group. In order to explore the effect of miR-132 on anxiety-like behavior of rats exposed to the SPS procedure, we

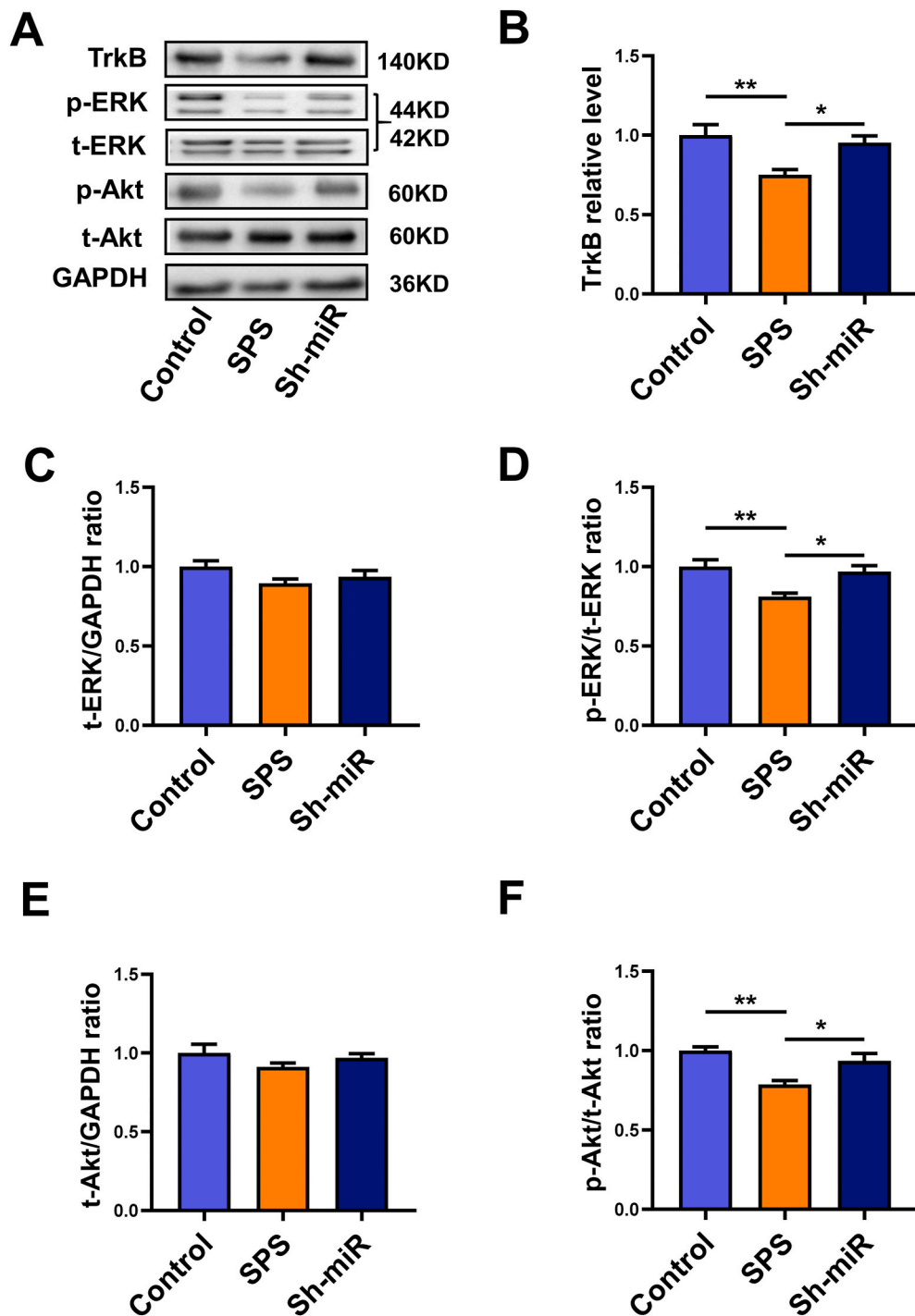


Fig. 5. The effect of anti-miR-132 on the expression of TrkB, ERK and Akt in the PFC. (A) Representative images of p-TrkB, t-TrkB, p-ERK and t-ERK in the PFC of rats in the Control, SPS or Sh-miR group. The ratio of (B) TrkB to GAPDH, (C) t-ERK to GAPDH, (D) p-ERK to t-ERK, (E) t-Akt to GAPDH and (F) p-Akt to t-Akt in the PFC of rats in each group. The data represent the means \pm standard errors of the mean (SEM) with 6 rats per group. GAPDH was used as a loading control. *P < 0.05, **P < 0.01.

injected miR-132 and anti-miR-132 carried by lentivirus through the lateral ventricle. The results showed that miR-132 downregulation could significantly reduce the anxiety-like symptoms in the rats exposed to SPS detected by EPM test. The mechanism by which anti-miR-132 could alleviate anxiety-like symptoms in the rats exposed to SPS has aroused our interest.

MiRNA may be assembled to recognize and bind the complementary sequence of mRNA and change protein translation or synthesis (Friedman et al., 2009). Our previous study has reported that anti-miR-132 could significantly alleviate anxiety and depression-like behavior through regulating the expression of synaptic protein via binding FXR1 (Nie et al., 2020). Indeed, it is unlikely that a single or a few miR-132

associated genes can fully explain the effect of it on regulating behaviors in rats exposed to SPS. Whether other genes in the CNS binding to miR-132 and related pathway are also involved in the formation of anxiety-like behaviors in the rats exposed to SPS need to be further explored. Next we predicted the probable target gene of miR-132-3p through bioinformatics analysis and found that *MeCP2*, which was highly expressed in the brain and involved in neuroplasticity (Fasolino and Zhou, 2017), was a target gene of it. Therefore, we tested the level of MeCP2 protein in the PFC of SPS rats. As expected, it was decreased significantly. We further confirmed that miR-132 could bind to the 3'UTR of *MeCP2* by dual luciferase reporter gene analysis. These results indicated that miR-132 might participate in the pathogenesis of PTSD by

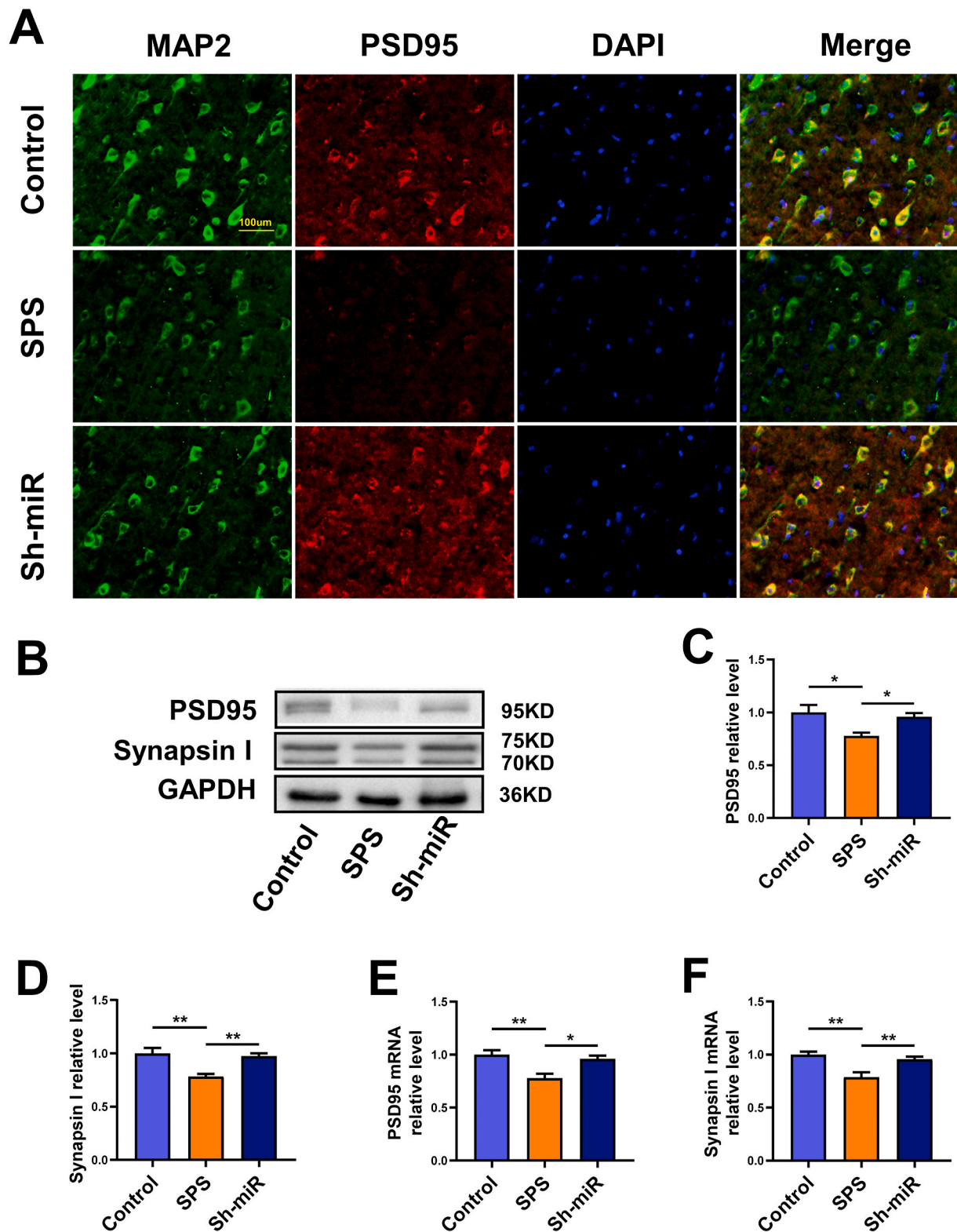


Fig. 6. The effect of anti-miR-132 on PSD95 expression in the PFC of rats exposed to SPS. (A) Representative images showing PSD95 and MAP2 immunopositive cells in the PFC of rats in the Control, SPS and sh-miR groups. (B) Representative bands of PSD95 and synapsin I protein tested by Western blot. The relative levels of (C) PSD95 and (D) synapsin I. Sample western blots for proteins are presented with GAPDH as a loading control. The relative levels of (E) PSD95 and (F) synapsin I mRNA tested by RT-qPCR. The data represent the means \pm standard errors of the mean (SEM). *P < 0.05.

binding to *MeCP2* mRNA, which could activate the expression of a variety of genes, as reported by many studies (Samaco and Neul, 2011; Yasui et al., 2007). The absence or duplication of *MeCP2* could change the density of dendrites and the morphology of dendritic spines, and it

could regulate synaptic characteristics through targets responsible for synaptic plasticity, such as BDNF. (Bertoldi et al., 2019; Na et al., 2013). The results of RT-qPCR and Western blot showed that the levels of both BDNF mRNA and protein in neuron-like cells was decreased by miR-132

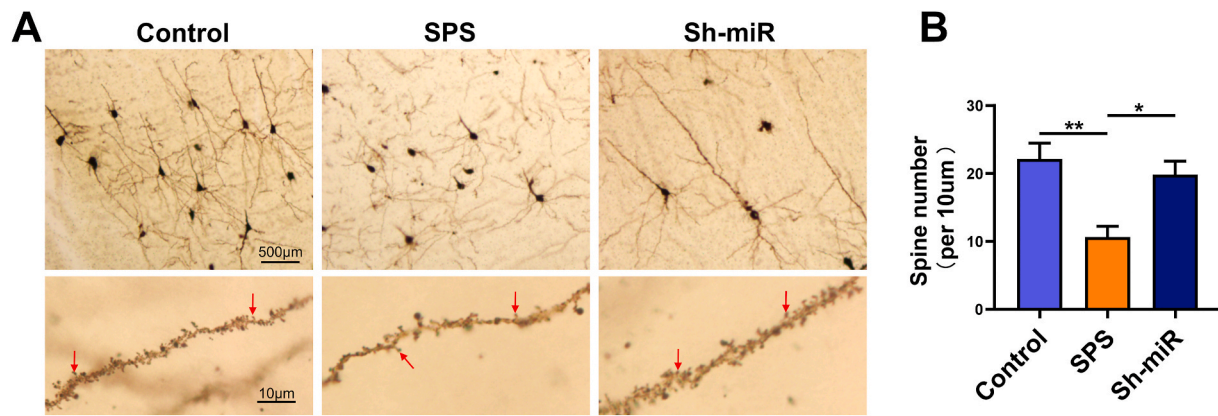


Fig. 7. The effect of miR-132 inhibition on the dendritic spine in the PFC of SPS rats. (A) Representative images of neurons in the PFC of rats in each group tested by Golgi staining. The red arrows indicate the dendritic spines of neurons. (B) The spine number of dendrites per 10 µm in each group. The data represent the means ± standard errors of the mean (SEM). *P < 0.05, **P < 0.01. (For interpretation of the references to colour in this figure legend, the reader is referred to the Web version of this article.)

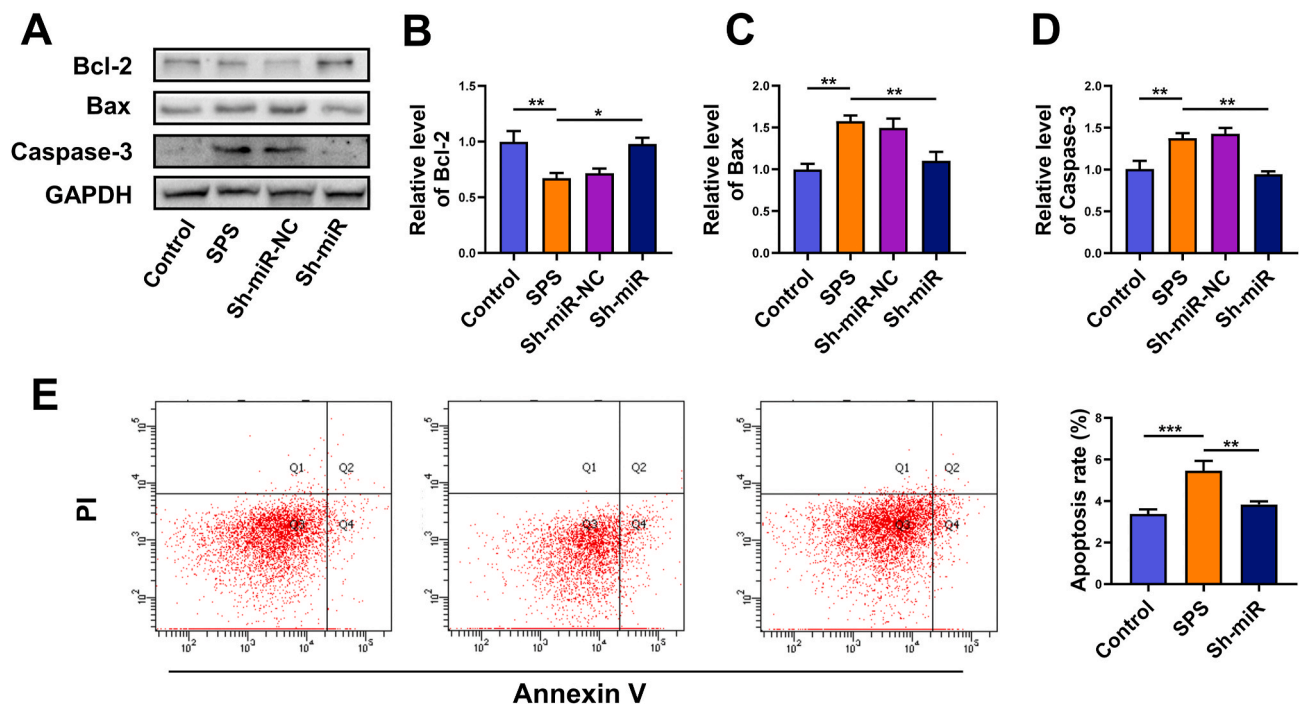


Fig. 8. The effects of miR-132 inhibition on the apoptosis of cells in the PFC of rats exposed to SPS. (A) Representative bands of Bcl-2, Bax and Caspase-3 protein. GAPDH was used as a loading control for Bcl-2, Bax, Caspase-3 and NF-κB p65 respectively. The relative levels of (B) Bcl-2, (C) Bax, (D) Caspase-3. (E) The ratio of apoptosis after transfection with miR-132 inhibitor in the PFC of the Control, SPS, Sh-miR-NC and Sh-miR groups. Bars indicate means ± SEM (n = 6). *P < 0.05, **P < 0.01, ***P < 0.001.

overexpression. Interestingly, different from the effect on cells, the injection of miR-132 did not further affect the expression of BDNF in the PFC of rats exposed to SPS. The difference between the in vivo and in vitro experiments may be due to the relatively complicated environment in vivo, but the specific reasons have not been studied clearly. However, BDNF was not a target gene of miR-132-3p according to the prediction of bioinformatics analysis. These increasing findings indicated that miR-132 might be one of the miRNAs that downregulated the level of MeCP2, which further upregulated the level of BDNF in the PFC of rats exposed to the SPS procedure.

Some studies have shown that low levels of BDNF and TrkB caused by chronic and acute stress could lead to dysregulation of neural development and neural plasticity, which was related to the pathogenesis of affective disorders (Luo et al., 2019). The interaction of BDNF and

TrkB improved neuronal differentiation and growth via activating ERK, and promoted neuronal survival by the activation of Akt (Minichiello, 2009). In the present study, anti-miR-132 might alleviate anxiety-like behaviors through upregulating the levels of BDNF and TrkB in the PFC, which might regulate the expression of PSD95 by regulating downstream signaling pathways. It has been reported that the formation of synapses and spine density depends on the level of the postsynaptic scaffold protein PSD95 and BDNF (Sen et al., 2017). The lower level of PSD95 and synapsin I in the PFC could be reversed by miR-132 downregulation in the present study, which indicated that miR-132 might influence the synaptic formation and spine density. We further found that both ERK and Akt pathway were activated by anti-miR-132 injection. This study showed that the indirect upregulation of BDNF by anti-miR-132 improved the expression of PSD95 and synapsin I through

activating ERK and Akt signaling pathway in the PFC of rats exposed to SPS.

It has been shown that miR-132 promoted the apoptosis of neural stem cells (Chen et al., 2018). In the present study, we also tested the levels of Bax and caspase-3 by western blotting, and the results showed that miR-132 downregulation could decrease the expression levels of the two proteins. The apoptosis rate of PFC neurons in SPS rats was also detected by flow cytometry, and the results showed that miR-132 inhibition could significantly decrease the apoptosis rate. However, it was unknown whether this effect of miR-132 inhibition was related to MeCP2, and the mechanism should be further studied in future experimental research.

Taken together, we found that anti-miR-132 injection could alleviate anxiety-like behavior through binding to the 3'UTR of MeCP2 mRNA, which further activated BDNF-TrkB pathway and its downstream factors, such as ERK and Akt, thereby regulating dendritic complexity and the expression of synaptic protein PSD95. Despite the above findings of this study we have completed, some limitations in the present study still need to be addressed. We should further detect the changes of MeCP2 and its downstream pathways in other two brain regions related to PTSD, including hippocampus and amygdala, and analyze the connections between these three brain regions to verify a therapeutic target in preventing anxiety-like behavior in the PTSD patients.

Funding

This work was supported by grants from the National Natural Science Foundation of China (No. 31900850), the Educational Commission of Liaoning Province, China (No. QN2019024) and National Undergraduate Innovation and Entrepreneurship Training Program (202010159029).

CRedit authorship contribution statement

Lei Tong: Conceptualization, Supervision, Writing – original draft, preparation. **Ming-Da Li:** Data curation, Investigation. **Peng-Yin Nie:** Methodology, Visualization. **Yao Chen:** Methodology, Software. **Yu-Lu Chen:** Methodology, Validation. **Li-Li Ji:** Funding acquisition, Project administration, Writing – review & editing.

Declaration of competing interest

The authors claim no conflict of interest.

References

- Armour, C., Contractor, A., Shea, T., Elhai, J.D., Pietrzak, R.H., 2016. Factor structure of the PTSD checklist for DSM-5: relationships among symptom clusters, anger, and impulsivity. *J. Nerv. Ment. Dis.* 204 (2), 108–115. <https://doi.org/10.1097/NMD.0000000000000430>.
- Bertoldi, M.L., Zalosnik, M.I., Fabio, M.C., Aja, S., Roth, G.A., Ronnett, G.V., Degano, A. L., 2019. MeCP2 deficiency disrupts kainate-induced presynaptic plasticity in the mossy fiber projections in the Hippocampus. *Front. Cell. Neurosci.* 13, 286. <https://doi.org/10.3389/fncel.2019.00286>.
- Bitencourt, R.M., Takahashi, R.N., 2018. Cannabidiol as a therapeutic alternative for post-traumatic stress disorder: from bench research to confirmation in human trials. *Front. Neurosci.* 12, 502. <https://doi.org/10.3389/fnins.2018.00502>.
- Briscone, M.A., Jovanovic, T., Norrholm, S.D., 2014. Conditioned fear associated phenotypes as robust, translational indices of trauma-, stressor-, and anxiety-related behaviors. *Front. Psychiatr.* 5, 88. <https://doi.org/10.3389/fpsy.2014.00088>.
- Bromis, K., Calem, M., Reinders, A., Williams, S.C.R., Kempton, M.J., 2018. Meta-analysis of 89 structural MRI studies in posttraumatic stress disorder and comparison with major depressive disorder. *Am. J. Psychiatr.* 175 (10), 989–998. <https://doi.org/10.1176/appi.ajp.2018.17111199>.
- Chen, D., Hu, S., Wu, Z., Liu, J., Li, S., 2018. The role of MiR-132 in regulating neural stem cell proliferation, differentiation and neuronal maturation. *Cell. Physiol. Biochem.* 47 (6), 2319–2330. <https://doi.org/10.1159/000491543>.
- Chen, W.G., Chang, Q., Lin, Y., Meissner, A., West, A.E., Griffith, E.C., Jaenisch, R., Greenberg, M.E., 2003. Derepression of BDNF transcription involves calcium-dependent phosphorylation of MeCP2. *Science* 302 (5646), 885–889. <https://doi.org/10.1126/science.1086446>.
- Cosentino, L., Vigli, D., Medici, V., Flor, H., Lucarelli, M., Fuso, A., De Filippis, B., 2019. Methyl-CpG binding protein 2 functional alterations provide vulnerability to develop behavioral and molecular features of post-traumatic stress disorder in male mice. *Neuropharmacology* 160, 107664. <https://doi.org/10.1016/j.neuropharm.2019.06.003>.
- Dajas-Bailador, F., Bonev, B., Garcez, P., Stanley, P., Guillemot, F., Papalopulu, N., 2012. microRNA-9 regulates axon extension and branching by targeting Map1b in mouse cortical neurons. *Nat. Neurosci.* 15 (5), 697–699. <https://doi.org/10.1038/nn.3082>.
- Dossi, G., Delvecchio, G., Prunas, C., Soares, J.C., Brambilla, P., 2020. Neural bases of cognitive impairments in post-traumatic stress disorders: a mini-review of functional magnetic resonance imaging findings. *Front. Psychiatr.* 11, 176. <https://doi.org/10.3389/fpsy.2020.00176>.
- Doxakis, E., 2010. Post-transcriptional regulation of alpha-synuclein expression by mir-7 and mir-153. *J. Biol. Chem.* 285 (17), 12726–12734. <https://doi.org/10.1074/jbc.M109.086827>.
- Eacker, S.M., Dawson, T.M., Dawson, V.L., 2013. The interplay of microRNA and neuronal activity in health and disease. *Front. Cell. Neurosci.* 7, 136. <https://doi.org/10.3389/fncel.2013.00136>.
- Fasolino, M., Zhou, Z., 2017. The crucial role of DNA methylation and MeCP2 in neuronal function. *Genes* 8 (5). <https://doi.org/10.3390/genes805041>.
- Femminella, G.D., Ferrara, N., Rengo, G., 2015. The emerging role of microRNAs in Alzheimer's disease. *Front. Physiol.* 6, 40. <https://doi.org/10.3389/fphys.2015.00040>.
- Friedman, R.C., Farh, K.K., Burge, C.B., Bartel, D.P., 2009. Most mammalian mRNAs are conserved targets of microRNAs. *Genome Res.* 19 (1), 92–105. <https://doi.org/10.1101/gr.082701.108>.
- Hou, L., Qi, Y., Sun, H., Wang, G., Li, Q., Wang, Y., Zhang, Z., Du, Z., Sun, L., 2018. Applying ketamine to alleviate the PTSD-like effects by regulating the HCN1-related BDNF. *Prog. Neuro-Psychopharmacol. Biol. Psychiatry* 86, 313–321. <https://doi.org/10.1016/j.pnpbp.2018.03.019>.
- Hu, Z., Li, Z., 2017. miRNAs in synapse development and synaptic plasticity. *Curr. Opin. Neurobiol.* 45, 24–31. <https://doi.org/10.1016/j.conb.2017.02.014>.
- Huang, E.J., Reichardt, L.F., 2003. Trk receptors: roles in neuronal signal transduction. *Annu. Rev. Biochem.* 72, 609–642. <https://doi.org/10.1146/annurev.biochem.72.121801.161629>.
- Jurkus, R., Day, H.L., Guimaraes, F.S., Lee, J.L., Bertoglio, L.J., Stevenson, C.W., 2016. Cannabidiol regulation of learned fear: implications for treating anxiety-related disorders. *Front. Pharmacol.* 7, 454. <https://doi.org/10.3389/fphar.2016.00454>.
- Kessler, R.C., Sonnega, A., Bromet, E., Hughes, M., Nelson, C.B., 1995. Posttraumatic stress disorder in the national comorbidity survey. *Arch. Gen. Psychiatr.* 52 (12), 1048–1060. <https://doi.org/10.1001/archpsyc.1995.03950240066012>.
- Klein, M.E., Li, D.T., Ma, L., Impey, S., Mandel, G., Goodman, R.H., 2007. Homeostatic regulation of MeCP2 expression by a CREB-induced microRNA. *Nat. Neurosci.* 10 (12), 1513–1514. <https://doi.org/10.1038/nn2010>.
- Krystal, J.H., Abdallah, C.G., Averill, L.A., Kelmendi, B., Harpaz-Rotem, I., Sanacora, G., Southwick, S.M., Duman, R.S., 2017. Synaptic loss and the pathophysiology of PTSD: implications for ketamine as a prototype novel therapeutic. *Curr. Psychiatr. Rep.* 19 (10), 74. <https://doi.org/10.1007/s11920-017-0829-z>.
- Lee, K.J., Kim, H., Kim, T.S., Park, S.H., Rhyu, I.J., 2004. Morphological analysis of spine shapes of Purkinje cell dendrites in the rat cerebellum using high-voltage electron microscopy. *Neurosci. Lett.* 359 (1–2), 21–24. <https://doi.org/10.1016/j.neulet.2004.01.071>.
- Luo, L., Li, C., Du, X., Shi, Q., Huang, Q., Xu, X., Wang, Q., 2019. Effect of aerobic exercise on BDNF/proBDNF expression in the ischemic hippocampus and depression recovery of rats after stroke. *Behav. Brain Res.* 362, 323–331. <https://doi.org/10.1016/j.bbr.2018.11.037>.
- Magill, S.T., Cambronne, X.A., Luikart, B.W., Li, D.T., Leighton, B.H., Westbrook, G.L., Mandel, G., Goodman, R.H., 2010. microRNA-132 regulates dendritic growth and arborization of newborn neurons in the adult hippocampus. *Proc. Natl. Acad. Sci. U. S. A.* 107 (47), 20382–20387. <https://doi.org/10.1073/pnas.1015691107>.
- Martinowich, K., Hattori, D., Wu, H., Fouse, S., He, F., Hu, Y., Fan, G., Sun, Y.E., 2003. DNA methylation-related chromatin remodeling in activity-dependent BDNF gene regulation. *Science* 302 (5646), 890–893. <https://doi.org/10.1126/science.1090842>.
- Matsushita, H., Morishita, R., Nata, T., Aoki, M., Nakagami, H., Taniyama, Y., Yamamoto, K., Higaki, J., Yasufumi, K., Ogihara, T., 2000. Hypoxia-induced endothelial apoptosis through nuclear factor-kappaB (NF-kappaB)-mediated bcl-2 suppression: in vivo evidence of the importance of NF-kappaB in endothelial cell regulation. *Circ. Res.* 86 (9), 974–981. <https://doi.org/10.1161/01.res.86.9.974>.
- Minichiello, L., 2009. TrkB signalling pathways in LTP and learning. *Nat. Rev. Neurosci.* 10 (12), 850–860. <https://doi.org/10.1038/nrn2738>.
- Na, E.S., Nelson, E.D., Kavalali, E.T., Monteggia, L.M., 2013. The impact of MeCP2 loss or gain-of-function on synaptic plasticity. *Neuropsychopharmacology* 38 (1), 212–219. <https://doi.org/10.1038/npp.2012.116>.
- Ni, L., Xu, Y., Dong, S., Kong, Y., Wang, H., Lu, G., Wang, Y., Li, Q., Li, C., Du, Z., Sun, H., Sun, L., 2020. The potential role of the HCN1 ion channel and BDNF-mTOR signaling pathways and synaptic transmission in the alleviation of PTSD. *Transl. Psychiatry* 10 (1), 101. <https://doi.org/10.1038/s41398-020-0782-1>.
- Nicholson, A.A., Sapru, I., Densmore, M., Frewen, P.A., Neufeld, R.W., Theberge, J., McKinnon, M.C., Lanius, R.A., 2016. Unique insula subregion resting-state functional connectivity with amygdala complexes in posttraumatic stress disorder and its dissociative subtype. *Psychiatry Res. Neuroimaging* 250, 61–72. <https://doi.org/10.1016/j.pscychres.2016.02.002>.
- Nie, P.Y., Ji, L.L., Fu, C.H., Peng, J.B., Wang, Z.Y., Tong, L., 2020. miR-132 regulates PTSD-like behaviors in rats following single-prolonged stress through fragile X-

- related protein 1. *Cell. Mol. Neurobiol.* <https://doi.org/10.1007/s10571-020-00854-x>.
- Reed, J.C., 1994. Bcl-2 and the regulation of programmed cell death. *J. Cell Biol.* 124 (1–2), 1–6. <https://doi.org/10.1083/jcb.124.1.1>.
- Roitbak, T., 2020. MicroRNAs and regeneration in animal models of CNS disorders. *Neurochem. Res.* 45 (1), 188–203. <https://doi.org/10.1007/s11064-019-02777-6>.
- Roskoski Jr., R., 2012. ERK1/2 MAP kinases: structure, function, and regulation. *Pharmacol. Res.* 66 (2), 105–143. <https://doi.org/10.1016/j.phrs.2012.04.005>.
- Samaco, R.C., Neul, J.L., 2011. Complexities of rett syndrome and MeCP2. *J. Neurosci.* 31 (22), 7951–7959. <https://doi.org/10.1523/JNEUROSCI.0169-11.2011>.
- Sen, T., Gupta, R., Kaiser, H., Sen, N., 2017. Activation of PERK elicits memory impairment through inactivation of CREB and downregulation of PSD95 after traumatic brain injury. *J. Neurosci.* 37 (24), 5900–5911. <https://doi.org/10.1523/JNEUROSCI.2343-16.2017>.
- Serova, L.I., Nwokafor, C., Van Bockstaele, E.J., Reyes, B.A.S., Lin, X., Sabban, E.L., 2019. Single prolonged stress PTSD model triggers progressive severity of anxiety, altered gene expression in locus coeruleus and hypothalamus and effected sensitivity to NPY. *Eur. Neuropsychopharmacol.* 29 (4), 482–492. <https://doi.org/10.1016/j.euroneuro.2019.02.010>.
- Shukla, G.C., Singh, J., Barik, S., 2011. MicroRNAs: processing, maturation, target recognition and regulatory functions. *Mol. Cell. Pharmacol.* 3 (3), 83–92.
- Siegel, G., Saba, R., Schratt, G., 2011. microRNAs in neurons: manifold regulatory roles at the synapse. *Curr. Opin. Genet. Dev.* 21 (4), 491–497. <https://doi.org/10.1016/j.gde.2011.04.008>.
- Sullivan, S.E., Jamieson, S., de Nijs, L., Jones, M., Snijders, C., Klengel, T., Joseph, N.F., Krauskopf, J., Kleinjans, J., Vinkers, C.H., Boks, M.P.M., Geuze, E., Vermetten, E., Berretta, S., Ressler, K.J., Rutten, B.P.F., Rumbaugh, G., Miller, C.A., 2020. MicroRNA regulation of persistent stress-enhanced memory. *Mol. Psychiatr.* 25 (5), 965–976. <https://doi.org/10.1038/s41380-019-0432-2>.
- Silva-Pena, D., Rivera, P., Alen, F., Vargas, A., Rubio, L., Garcia-Marchena, N., Pavon, F. J., Serrano, A., Rodriguez de Fonseca, F., Suarez, J., 2019. Oleylethanolamide modulates BDNF-ERK signaling and neurogenesis in the hippocampi of rats exposed to delta(9)-THC and ethanol binge drinking during adolescence. *Front. Mol. Neurosci.* 12, 96. <https://doi.org/10.3389/fnmol.2019.00096>.
- Smalheiser, N.R., Lugli, G., Rizavi, H.S., Torvik, V.I., Turecki, G., Dwivedi, Y., 2012. MicroRNA expression is down-regulated and reorganized in prefrontal cortex of depressed suicide subjects. *PLoS One* 7 (3), e33201. <https://doi.org/10.1371/journal.pone.0033201>.
- Snijders, C., de Nijs, L., Baker, D.G., Hauger, R.L., van den Hove, D., Kenis, G., Nievergelt, C.M., Boks, M.P., Vermetten, E., Gage, F.H., Rutten, B.P.F., 2018. MicroRNAs in post-traumatic stress disorder. *Curr. Top Behav. Neurosci.* 38, 23–46. https://doi.org/10.1007/7854_2017_32.
- Wanet, A., Tachenay, A., Arnould, T., Renard, P., 2012. miR-212/132 expression and functions: within and beyond the neuronal compartment. *Nucleic Acids Res.* 40 (11), 4742–4753. <https://doi.org/10.1093/nar/gks151>.
- Wayman, G.A., Davare, M., Ando, H., Fortin, D., Varlamova, O., Cheng, H.Y., Marks, D., Obrietan, K., Soderling, T.R., Goodman, R.H., Impey, S., 2008. An activity-regulated microRNA controls dendritic plasticity by down-regulating p250GAP. *Proc. Natl. Acad. Sci. U. S. A.* 105 (26), 9093–9098. <https://doi.org/10.1073/pnas.0803072105>.
- Wei, Z., Mahaman, Y.A.R., Zhu, F., Wu, M., Xia, Y., Zeng, K., Yang, Y., Liu, R., Wang, J.Z., Shu, X., Wang, X., 2019. GSK-3beta and ERK1/2 incongruously act in tau hyperphosphorylation in SPS-induced PTSD rats. *Aging (Albany NY)* 11 (18), 7978–7995. <https://doi.org/10.18632/aging.102303>.
- Yasui, D.H., Peddada, S., Bieda, M.C., Vallero, R.O., Hogart, A., Nagarajan, R.P., Thatcher, K.N., Farnham, P.J., Lasalle, J.M., 2007. Integrated epigenomic analyses of neuronal MeCP2 reveal a role for long-range interaction with active genes. *Proc. Natl. Acad. Sci. U. S. A.* 104 (49), 19416–19421. <https://doi.org/10.1073/pnas.0707442104>.
- Zhou, Z., Hong, E.J., Cohen, S., Zhao, W.N., Ho, H.Y., Schmidt, L., Chen, W.G., Lin, Y., Savner, E., Griffith, E.C., Hu, L., Steen, J.A., Weitz, C.J., Greenberg, M.E., 2006. Brain-specific phosphorylation of MeCP2 regulates activity-dependent Bdnf transcription, dendritic growth, and spine maturation. *Neuron* 52 (2), 255–269. <https://doi.org/10.1016/j.neuron.2006.09.037>.